

## Measurement of neutron multiplicity to investigate the role of entrance channel parameters on the nuclear dissipation

N. K. Rai,\* A. Gandhi, and Ajay Kumar

*Department of Physics, Banaras Hindu University, Varanasi-221005, India*

N. Saneesh, M. Kumar, G. Kaur, A. Parihari, D. Arora, K. S. Golda, A. Jhingan, and P. Sugathan

*Inter University Accelerator Centre, New Delhi-110067, India*

T. K. Ghosh and Jhilm Sadhukhan

*Variable Energy Cyclotron Centre, 1/AF Bidhan Nagar, Kolkata-700064, India*

B. K. Nayak

*Nuclear Physics Division, Bhabha Atomic Research Centre, Mumbai-400085, India*

Nabendu K. Deb

*Department of Physics, Gauhati University, Guwahati-781014, Assam, India*

S. Biswas and A. Chakraborty

*Department of Physics, Siksha Bhavana, Visva-Bharati, Santiniketan, West Bengal-731235, India*



(Received 6 March 2019; revised manuscript received 14 June 2019; published 24 July 2019)

In the present work, the pre- and post-scission neutron multiplicities were measured for the reaction  $^{18}\text{O} + ^{186}\text{W}$  at different excitation energies populating the compound nucleus  $^{204}\text{Pb}$ , using the National Array of Neutron Detectors (NAND) facility at IUAC, New Delhi, India. Here, we investigated the entrance channel effect on the nuclear dissipation involved in the heavy ion fusion-fission dynamics. The statistical model analysis was performed using the code VECSTAT. The prescribed reaction  $^{18}\text{O} + ^{186}\text{W}$  had similar value of the mass asymmetry as the system  $^{16}\text{O} + ^{181}\text{Ta}$  studied earlier, populating the compound nucleus  $^{197}\text{Tl}$ . Specifically, we observed the similar behavior from both the systems against the nuclear dissipation, with the similar value of the mass asymmetry. The role of the entrance channel parameters on the nuclear dissipation was also discussed in the present work.

DOI: [10.1103/PhysRevC.100.014614](https://doi.org/10.1103/PhysRevC.100.014614)

### I. INTRODUCTION

The study of heavy-ion induced fusion-fission reactions is an interesting topic in the domain of nuclear physics, investigated by theoretical as well as experimental approaches. Here, the projectile is captured by the target nucleus and a compound nucleus (CN) is formed, equilibrated in all degrees of freedom. The fusion-fission process of the excited compound nucleus can be understood by the evaporation of particles such as alpha, proton, neutron, gamma, and fission fragments. In the collision between two heavy nuclei, quasifission as well as fusion-fission have a considerable contribution in the process. The measurement of the pre-scission multiplicity of light charged particles [1,2], the neutrons [3–5], and GDR  $\gamma$  rays [6,7], evaporation residue cross sections [8,9], and the mass and angular distribution of the fission fragments [10,11] are well-established tools to understand the heavy-ion induced fusion-fission process.

In the fusion-fission process, dynamical effect plays a crucial role, slowing down the decay process of the CN. To understand the fission hindrance, the multiplicity of the different type of particles is experimentally measured, which is higher than the standard statistical model predictions [12,13]. The excess yield of the particle multiplicity from the heavy compound system indicates the slowing down of the fission process, described by the transition-state model of the fission [14]. The slowing down of the fission process or fission hindrance can be understood incorporating the concept of the nuclear dissipation. The dynamical effects are present in the decay of CN from the presence of nuclear viscosity. The nuclear dissipation is one-body in nature [15], which is described by incorporating the concept of wall and window friction. Fission delay time is also calculated for the excess pre-scission neutrons [10,16], directly related to the magnitude of the nuclear dissipation.

Nuclear dissipation is one of the most interesting topics in nuclear physics at the lower and intermediate energy. Nuclear dissipation is caused by the the coupling of the collective

\*nkrai233231@gmail.com

motion with the particle degrees of freedom in the mean-field nuclear dynamics. Apart from the nuclear dissipation, fission timescale depends on the shell effects in fission barrier height and the density of the nuclear levels [8,17]. In the experimental measurements of heavy-ion induced fusion-fission reactions, shell effect plays an important role. Neutron multiplicity measurements are reported to observe the effect of shell closure on the nuclear dissipation [18–20]. The measurements of pre-scission neutron multiplicity are done for the compound nuclei with same  $Z$  but different  $N$  values [18,21,22]. It has also been investigated theoretically that the dissipation strength is sensitive with respect to the  $N/Z$  ratio [23,24]. However, the experimentally measured neutron multiplicity spectra does not show any specific trends with respect to the  $N/Z$  ratio [20,25]. Pre-scission neutron multiplicity is measured for the two different reaction channels populating the same compound nucleus at the same excitation energy. Neutron multiplicity is higher for the more symmetric reactions, which represents that nuclear dissipation depends on the entrance channel [26,27].

Influence of fusion dynamics on the fission observables was studied dealing with the effect of the entrance channel mass asymmetry, bombarding energy, angular momentum, and excitation energy imparted to the compound nucleus [28]. It was observed that to develop a unified model of the fusion-fission dynamics further measurements are needed, and to discriminate the role of the fusion and fission dynamics a large set the experimental data is required. The statistical model analysis was performed for the neutron multiplicity; data are available in the literature. The higher value of the neutron multiplicity was observed for more symmetric reactions in comparison with the asymmetric reactions forming the same compound nucleus; in a few cases, a reverse trend was also observed [29]. These observations suggest more neutron multiplicity measurement to study the entrance channel dependency, and to understand the systematics of the fusion-fission reactions. In the present work, we have experimentally measured the pre- and post-scission neutron multiplicity for the reaction  $^{18}\text{O} + ^{186}\text{W}$  populating the CN  $^{204}\text{Pb}$  at the three excitation energies 78.92 MeV, 74.36 MeV, and 69.80 MeV. Here, we have selected the reaction  $^{18}\text{O} + ^{186}\text{W}$  because it has the nearly same value of entrance channel mass asymmetry as the earlier studied system  $^{16}\text{O} + ^{181}\text{Ta}$  [26] populating the CN  $^{197}\text{Tl}$ . Therefore, the present study can describe the effect of entrance channel parameters on the nuclear dissipation by measuring the pre-session neutron multiplicity.

## II. EXPERIMENTAL DETAILS

The experiment was performed using the National Array of Neutron Detectors (NAND) facility at Beam Hall-II of the Inter University Accelerator Center (IUAC), New Delhi, India. The pulsed beam of  $^{18}\text{O}$  with a repetition rate of 250 ns delivered from 15UD Pelletron accelerator was bombarded on  $^{186}\text{W}$  target of thickness  $637 \mu\text{g}/\text{cm}^2$  with carbon backing of  $40 \mu\text{g}/\text{cm}^2$ . The target was prepared by the evaporation method, where the tungsten material was evaporated on the carbon substrate. The target was placed in the center of a

spherical shaped scattering chamber of 1-m diameter on the target ladder, which can move in the vertical directions.

The fission fragments were detected using a pair of the multiwire proportional counters (MWPCs) of active area  $11 \times 16 \text{ cm}^2$ , placed at the folding angle. First MWPC was placed in the forward direction at the distance of 26 cm ( $35^\circ$ ) and another was in the backward direction at distance of 21 cm ( $126^\circ$ ) from the target, where angles are considered with respect to the beam directions. MWPCs were operated with isobutane gas at gas pressure of 4 mbar. The time-of-flight (TOF) information of the fission fragments were obtained using the fast timing signal of the MWPCs with reference to the beam arrival time. Using the TOF signal, fission fragment events were separated from the other competing channels. Two silicon surface barrier detectors (SSBD) were also placed inside the chamber at  $\pm 12.5^\circ$  with respect to the beam directions to monitor the beam.

The neutrons emitted from the CN and fission fragments were detected using the organic liquid scintillator (BC 501) detectors of the NAND facility [30,31]. The array consists of 100 neutron detectors placed at a different polar  $\theta$  and azimuthal  $\phi$  angles in the configuration of semispherical shape with a fixed radius of 175 cm [32]. The cylindrical neutron detector dimension was 5 inch  $\times$  5 inch. The flight path of the detectors from the target position was 175 cm. The array contains eight rings on the semispherical dome, where the eighth ring corresponds to the  $15^\circ$  below the reaction plane. In the reaction plane, 16 detectors were kept ranging from  $18^\circ$  to  $342^\circ$  and the remaining 84 detectors were out of the reaction plane. The threshold for the neutron detectors was kept at about 0.5 MeV by calibrating with the standard gamma sources ( $^{137}\text{Cs}$  and  $^{60}\text{Co}$ ) [33]. The neutrons were discriminated using the pulse shape discrimination (PSD) based on the zero crossing and TOF technique [34]. The neutron TOF spectra were converted into the energy spectra by considering the prompt  $\gamma$  peak as the reference line. To reduce the background, the beam dump was placed 4 m downstream from the target and it was shielded with paraffin and lead bricks. A blank run was also taken to estimate the level of background in the neutron spectra, which was found to be negligible. The neutron detector efficiency used in the experiment was measured experimentally by using the  $^{252}\text{Cf}$  source kept at the target position.

The data were collected in the event-by-event mode using the VME-based data acquisition system based on the LAMPS (Linux Advanced Multi-Parameter System) software. The data acquisition was triggered by making the coincidence between the RF of the beam pulse and OR of the MWPCs.

## III. DATA ANALYSIS AND RESULTS

The neutron TOF spectra were converted into energy spectra by using the relation,

$$E_n = \frac{1}{2} m_n \left( \frac{d}{t} \right)^2, \quad (1)$$

where  $E_n$  is neutron energy,  $m_n$  is neutron mass,  $d$  is the distance between target and detector, and  $t$  is the neutron TOF. The pre- and post-scission components of the neutron

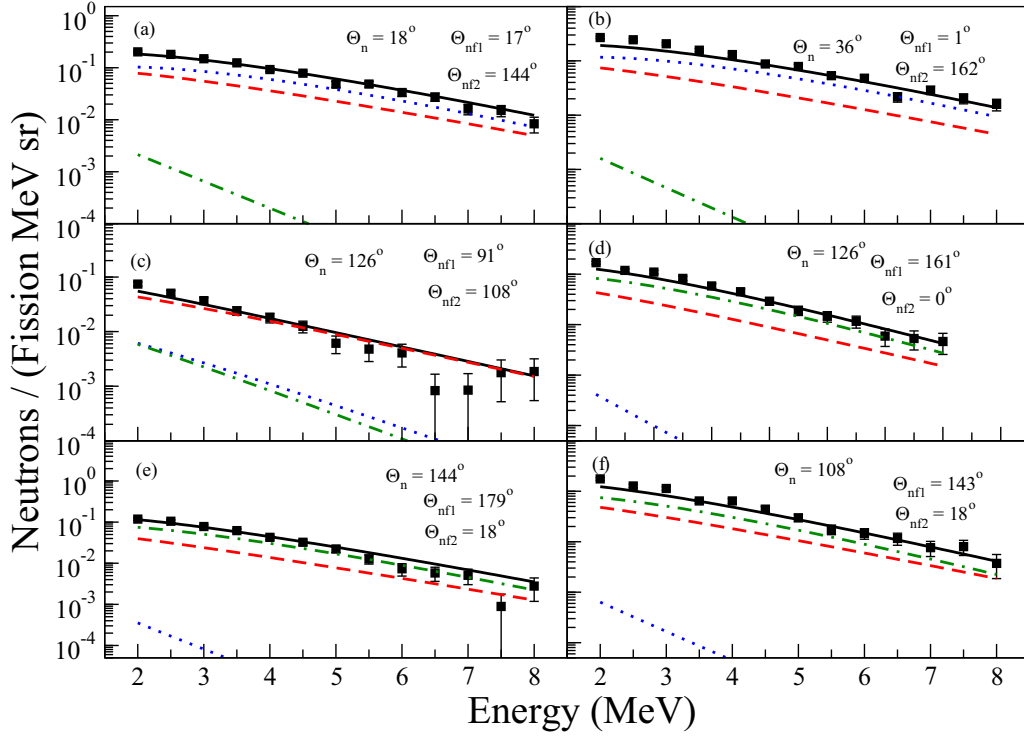


FIG. 1. Neutron multiplicity spectra (filled squares) at various angles for the reaction  $^{18}\text{O} + ^{186}\text{W}$  at  $E_{\text{lab}} = 106.51$  MeV along with the fits for the pre-scission (dashed lines) and post-scission contributions from the one fragment (dotted lines) and that from the other (dotted-dash lines) are shown. Here, the solid black line represents the total contribution.

multiplicities were extracted from the experimentally measured neutron energy spectra. Fitting was done using the Watt expression [12] by the procedure of multiple source least-square fitting, which is given as

$$\frac{d^2 M_n}{dE_n d\Omega_n} = \sum_{i=1}^3 \frac{M_n^i \sqrt{E_n}}{2(\pi T^i)^{3/2}} \times \exp \left[ -\frac{E_n - 2\sqrt{E_n E^i/A^i} \cos \theta^i + E^i/A^i}{T^i} \right]. \quad (2)$$

There are three sources of neutrons: pre-scission neutrons are emitted from the compound nucleus and post-scission neutrons are emitted from the fully accelerated fission fragments. In Eq. (2),  $E_n$  is the energy of emitted neutrons in the laboratory frame and  $A^i$ ,  $E^i$ ,  $T^i$ , and  $M_n^i$  are, respectively, the mass, energy, temperature, and multiplicity of each neutron emitting source. The emitted neutrons from these moving sources are assumed to be isotropic in their respective rest frames. The energy of fission fragments and folding angles were obtained from the Viola systematics for the symmetric fission [35]. To avoid any angular uncertainty, fission events are only selected in the range of  $\pm 6.5^\circ$  from the central position of the MWPCs. Pre- and post-scission neutron multiplicities and temperatures, denoted, respectively, as  $M^{\text{pre}}$ ,  $M^{\text{post}}$ ,  $T^{\text{pre}}$ , and  $T^{\text{post}}$  were determined by least-square fitting considering them as free parameters.  $M^{\text{post}}$  and  $T^{\text{post}}$  were considered to be equal for both the fission fragments by assuming the fission

process completely symmetric. The total neutron multiplicity  $M^{\text{tot}}$  can be written as the sum of  $M^{\text{pre}}$  and two times of  $M^{\text{post}}$  as

$$M^{\text{tot}} = M^{\text{pre}} + 2 \times M^{\text{post}}. \quad (3)$$

Fitted plots to the double differential neutron multiplicity spectra at various angles for the reaction  $^{18}\text{O} + ^{186}\text{W}$  at 106.51 MeV are shown in Fig. 1 and values of all the multiplicities and temperatures are given in Table I.

The total double differential neutron spectra, as a contribution from different neutron emitting sources, depends on the laboratory angles with respect to the beam direction. Measurements are made at various fission-neutron correlation angles; because of the effect of kinematic focusing for fragment emission pre- and post-components are separated. It was observed in Fig. 1 that the post-scission contributions are dominant at the angle around  $0^\circ$ . We have plotted the pre-scission and total neutron multiplicity for the reaction  $^{18}\text{O} + ^{186}\text{W}$  at different excitation energies as shown in Fig. 2. The value of  $M^{\text{pre}}$  and  $M^{\text{tot}}$  increases with increasing value of the excitation energy of the CN.

The pre-scission neutron emission probability is approximately given as  $\frac{\Gamma_n}{\Gamma_f} \approx \exp^{-(B_n - V_B)/T}$ , where  $\Gamma_n$  and  $\Gamma_f$  are neutron emission and fission decay widths,  $B_n$  and  $V_B$  are neutron binding energy and fission barrier, respectively, and  $T$  is the compound nucleus temperature. The fission barrier height decreases with increasing value of the excitation energy of the compound nucleus, and for  $B_n > V_B$  neutron emission probability increases with  $T$ .

TABLE I. Experimentally measured values of neutron multiplicities and temperatures for the reaction  $^{18}\text{O} + ^{186}\text{W}$ .

$E_{\text{lab}}$ (MeV)	$E_{\text{CN}}^*$ (MeV)	$M^{\text{pre}}$	$M^{\text{post}}$	$M^{\text{tot}}$	$T^{\text{pre}}$	$T^{\text{post}}$
96.49	69.80	$2.14 \pm 0.25$	$1.27 \pm 0.09$	$4.68 \pm 0.31$	$1.51 \pm 0.12$	$0.98 \pm 0.05$
101.50	74.36	$2.47 \pm 0.22$	$1.17 \pm 0.08$	$4.81 \pm 0.27$	$1.55 \pm 0.09$	$0.98 \pm 0.05$
106.51	78.92	$3.09 \pm 0.26$	$1.06 \pm 0.10$	$5.21 \pm 0.28$	$1.57 \pm 0.08$	$0.98 \pm 0.06$

#### IV. THEORETICAL CALCULATIONS

We have estimated the values of  $M^{\text{pre}}$  and  $M^{\text{post}}$  for the reaction  $^{18}\text{O} + ^{186}\text{W}$  using the statistical model calculation (VECSTAT) [36]. The statistical model considers the emission of light charged particle, neutron, GDR  $\gamma$  rays, and fission of the compound nucleus. The partial decay width of the light particle and GDR  $\gamma$  rays were obtained from the Weisskopf formula [37]. The dynamics of the fission degrees of freedom are considered similar to the Brownian particle in a heat bath and fission width is calculated from the work of Kramers [38]. The compound nucleus temperature  $T$  is considered as the temperature of the heat bath corresponding to all the nuclear degrees of freedom. The hot nucleus is driven by the force provided by the free energy of the system [39,40], which is given by the Fermi gas model as

$$F(q, T) = V(q) - a(q)T^2, \quad (4)$$

where  $q$  is the collective coordinates,  $V(q)$  is collective potential obtained from the finite-range liquid drop model (FRLDM)[41], and  $a(q)$  is the level density parameter, which is dependent on the shape of the compound nucleus. The Kramer's fission width is written as [38,42]

$$\Gamma_K = \frac{\hbar\omega_g}{2\pi} \exp\left(\frac{-V_B}{T}\right) \left( \sqrt{1 + \left(\frac{\beta}{2\omega_s}\right)^2} - \frac{\beta}{2\omega_s} \right), \quad (5)$$

where  $\beta$  is the dissipation coefficient,  $V_B$  is the fission barrier in the free energy profile, and  $\omega_g$ , and  $\omega_s$  are the frequency of a harmonic oscillator potential at ground state and saddle configuration, respectively.

During the decay process of CN, the Kramers's fission width is a stationary fission rate, therefore a time-dependent fission width is used to account for the transient time, which

passes off before the stationary value of the Kramer's modified width is reached. It is introduced in the statistical model by using a parametrized form of the dynamical fission width, which is written as [43]

$$\Gamma_f(t) = \Gamma_K[1 - \exp(-2.3t/\tau_f)], \quad (6)$$

where

$$\tau_f = \frac{\beta}{2\omega_g^2} \ln\left(\frac{10V_B}{T}\right)$$

is the transient time period. The stability of the CN is decided by the relative magnitude of the various decay channels in the statistical model. After the emission of light particles and  $\gamma$  rays, a residual nucleus is formed having new excitation energy and angular momentum. This process remains to continue until either the compound nucleus undergoes fission or an evaporation residue is formed. In the case of fission, further emission can take place during the transition from the saddle to scission, which contributes to the pre-scission multiplicities. This saddle-to-scission time interval is given as [44]

$$\tau_{ss} = \tau_{ss}^0 \left( \sqrt{1 + \left(\frac{\beta}{2\omega_s}\right)^2} + \frac{\beta}{2\omega_s} \right), \quad (7)$$

where  $\tau_{ss}^0$  is the nondissipative saddle-to-scission time interval [45].

In the present work, we have performed the statistical model calculation and statistical model predicts the different values of  $M^{\text{pre}}$  with different values of  $\beta$  as shown in Fig. 3.

Statistical model predictions with  $\beta = 0 \text{ s}^{-1}$  are found to underestimate the experimental value of  $M^{\text{pre}}$  as shown

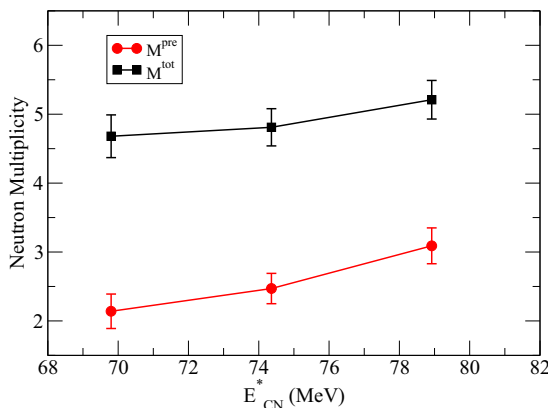


FIG. 2. Experimental values of pre-scission and total neutron multiplicity for the reaction  $^{18}\text{O} + ^{186}\text{W}$ .

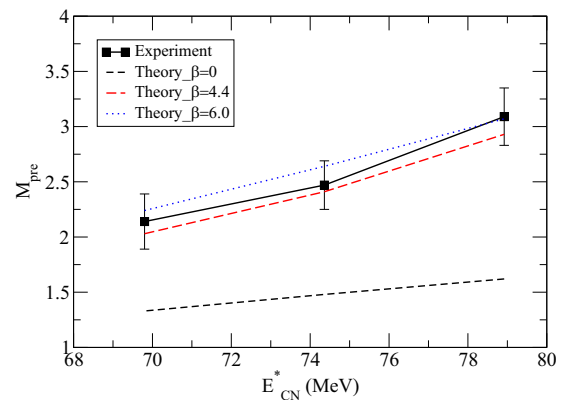


FIG. 3. Experimental values of pre-scission neutron multiplicities for the reaction  $^{18}\text{O} + ^{186}\text{W}$  and their comparison with the statistical model predictions.

in Fig. 3. The experimentally measured value of the  $M^{\text{pre}}$  is perfectly estimated by the statistical model providing the dissipation parameter in the range of  $\beta = (4.4\text{--}6.0) \times 10^{21} \text{ s}^{-1}$ . In our earlier work, neutron multiplicity was measured for the same compound nucleus populated with two different entrance channels. The experimentally measured neutron multiplicity for the symmetric entrance channel was higher compared to the asymmetric entrance channel [27]. It was concluded that the formation time of CN is entrance channel dependent and is higher for the symmetric systems compared to the asymmetric systems. Therefore, the higher value of the dissipation coefficient  $\beta$  is required in case of the more symmetric systems compared to the asymmetric systems. The nuclear dissipation slows down the fusion-fission process and results in the increment in the neutron multiplicity during the evolution of the CN. Because the statistical model considers the pre-scission neutron multiplicity after the formation of the compound nucleus, but in the experimentally measured values of neutron multiplicity, neutrons emitted during the formation of the compound nucleus also have a significant contribution [27].

Here, we have matched the entrance channel mass asymmetry  $\alpha = (A_t - A_p)/(A_t + A_p)$ , of the reaction  $^{18}\text{O} + ^{186}\text{W}$  ( $\alpha = 0.824$ ) with the already studied system  $^{16}\text{O} + ^{181}\text{Tl}$  [26] ( $\alpha = 0.838$ ). The similar excitation energy for the reaction  $^{18}\text{O} + ^{186}\text{W}$  is 70 MeV, which is matching with the 72 MeV of the reaction  $^{16}\text{O} + ^{181}\text{Ta}$ . We have also calculated the formation time,  $t_{\text{form}}$  using the dynamical model calculation (HICOL) [46]. The value of formation time ( $t_{\text{form}} \approx 25 \times 10^{-22} \text{ s}$ ) is almost the same for both the systems. The reactions  $^{18}\text{O} + ^{186}\text{W}$  and  $^{16}\text{O} + ^{181}\text{Ta}$  are populating the different CN, therefore pre-scission neutron multiplicity will be different. The value of the pre-scission neutron multiplicity is calculated using the SM for the reaction  $^{16}\text{O} + ^{181}\text{Tl}$ . It was found that the  $\beta = 4.8 \times 10^{21} \text{ s}^{-1}$  was required to get the experimental value for the reaction  $^{16}\text{O} + ^{181}\text{Tl}$ , which is in the range as required for reaction  $^{18}\text{O} + ^{186}\text{W}$ . This shows that for the reactions  $^{18}\text{O} + ^{186}\text{W}$  and  $^{16}\text{O} + ^{181}\text{Tl}$  (having the similar value of entrance channel mass asymmetry  $\alpha$  and formation time  $t_{\text{form}}$ ) the value of dissipation parameter  $\beta$  is almost similar, which concludes that  $\beta$  is dependent on the entrance channel mass asymmetry  $\alpha$ . This observation is providing a relation between the nuclear dissipation with the entrance channel mass asymmetry for the present study.

To understand how the mass asymmetry is affecting the nuclear dissipation in the fusion-fission process, we have

TABLE II. The entrance channel parameters for the reactions considered for the analysis in this work.

Reaction	CN	$E^*$ (MeV)	$\alpha$	$Z_p Z_T$	Ref.
$^{48}\text{Ti} + ^{154}\text{Sm}$	$^{202}\text{Po}$	72	0.525	1364	[25]
$^{28}\text{Si} + ^{175}\text{Lu}$	$^{203}\text{At}$	73	0.724	994	[3]
$^{19}\text{F} + ^{184}\text{W}$	$^{203}\text{Bi}$	74	0.813	666	[47]
$^{18}\text{O} + ^{186}\text{W}$	$^{204}\text{Pb}$	70	0.824	592	Present work
$^{16}\text{O} + ^{181}\text{Ta}$	$^{197}\text{Tl}$	72	0.837	584	[26]
$^{12}\text{C} + ^{194}\text{Pt}$	$^{206}\text{Po}$	76	0.883	468	[48]

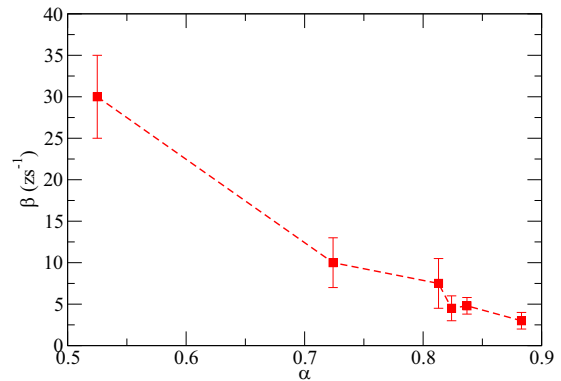


FIG. 4. Variation of the dissipation parameter  $\beta$  with respect to the entrance channel mass asymmetry  $\alpha$ .

chosen some already studied systems in the literature, populating the compound nucleus at near value of the mass number and excitation energy. The reactions are shown in Table II. We have performed the statistical model calculation for the above mentioned systems, and the calculated value of the  $M^{\text{pre}}$  is matched with their experimental value by changing the dissipation parameter  $\beta$ . The required value of the dissipation parameter  $\beta$  is plotted with respect to the entrance channel mass asymmetry, which is shown in Fig. 4 and from the same figure it is pointed out that for the lower value of the mass asymmetry higher value of the dissipation parameter is required.

Here, it can be seen that the nuclear dissipation decreases with the increasing value of the mass asymmetry.

In Ref. [49], it was mentioned that during the formation of the compound nucleus, nuclear dissipation depends on the Coulomb factor  $Z_p Z_T$ , and it increases with the increasing value of the  $Z_p Z_T$ . Because at the higher excitation energy the maximum contribution of the neutron multiplicity is from the formation process therefore we have tried to verify this theoretical investigation. For this purpose we have used the above mentioned systems as shown in Table II. The required value of the dissipation parameter  $\beta$  is plotted with respect to the Coulomb factor  $Z_p Z_T$ , which is shown in Fig. 5 and

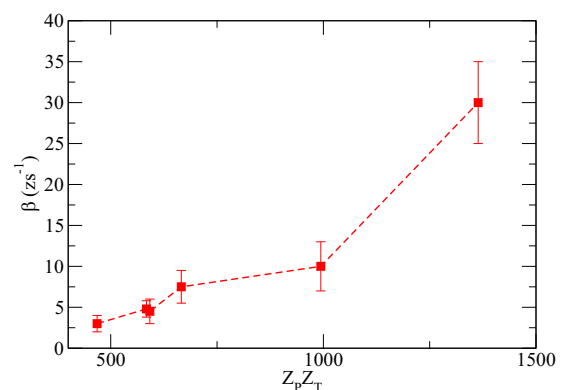


FIG. 5. Variation of the dissipation parameter  $\beta$  with respect to the Coulomb factor  $Z_p Z_T$ .

it can be concluded that in the fusion-fission process, nuclear dissipation increases with the increasing value of the Coulomb factor.

## V. CONCLUSION

In this work, we have measured the pre- and post-scission neutron multiplicity for the reaction  $^{18}\text{O} + ^{186}\text{W}$ . We have compared our results with the system  $^{16}\text{O} + ^{181}\text{Ta}$ , existing in the literature. It was found that for the similar value of the entrance channel mass asymmetry at the same excitation energy, populating the compound nucleus in same mass region, almost similar value of the dissipation parameter is required. Moreover, we have chosen the different systems from the literature with different mass asymmetry, populating the compound nucleus with near value of mass number and excitation energy. The required value of the dissipation parameter to match the statistical model predicted value of  $M^{\text{pre}}$  with the experimental value is higher for the lower value of

the entrance channel mass asymmetry. It concludes that in the fusion-fission process, nuclear dissipation decreases with the increasing value of the entrance channel mass asymmetry. In the present case, it was also verified that nuclear dissipation increases with the increasing value of the Coulomb factor  $Z_P Z_T$  as mentioned in the theoretical article [49].

## ACKNOWLEDGMENTS

The authors would like to thank the Pelletron accelerator staff of IUAC, New Delhi for providing the excellent quality beam and their careful work. The authors are also grateful to Dr. A. Chatterjee for providing the moving source code. One of the authors (A.K.) thanks the IUAC-UGC, Government of India (Sanction No. IUAC/XIII.7/UFR-58310), DST, Government of India (Sanction No. INT/RUS/RFBR/P-250), and DAE-BRNS, Government of India (Sanction No. 36(6)/14/23/2016-BRNS) for financial support for this work.

- 
- [1] J. P. Lestone, *Phys. Rev. Lett.* **70**, 2245 (1993).
- [2] H. Rossner, D. Hilscher, D. J. Hinde, B. Gebauer, M. Lehmann, M. Wilpert, and E. Mordhorst, *Phys. Rev. C* **40**, 2629 (1989).
- [3] K. Ramachandran, A. Chatterjee, A. Navin, K. Mahata, A. Shrivastava, V. Tripathi, S. Kailas, V. Nanal, R. G. Pillay, A. Saxena, R. G. Thomas, S. Kumar, and P. K. Sahu, *Phys. Rev. C* **73**, 064609 (2006).
- [4] J. Cabrera, T. Keutgen, Y. El Masri, C. Dufauquez, V. Roberfroid, I. Tilquin, J. Van Mol, R. Régimbart, R. J. Charity, J. B. Natowitz, K. Hagel, R. Wada, and D. J. Hinde, *Phys. Rev. C* **68**, 034613 (2003).
- [5] D. J. Hinde, D. Hilscher, H. Rossner, B. Gebauer, M. Lehmann, and M. Wilpert, *Phys. Rev. C* **45**, 1229 (1992).
- [6] I. Dio'szegi, N. P. Shaw, I. Mazumdar, A. Hatzikoutelis, and P. Paul, *Phys. Rev. C* **61**, 024613 (2000).
- [7] I. Dio'szegi, N. P. Shaw, A. Bracco, F. Camera, S. Tettoni, M. Mattiuzzi, and P. Paul, *Phys. Rev. C* **63**, 014611 (2000).
- [8] B. B. Back, D. J. Blumenthal, C. N. Davids, D. J. Henderson, R. Hermann, D. J. Hofman, C. L. Jiang, H. T. Penttila, and A. H. Wuosmaa, *Phys. Rev. C* **60**, 044602 (1999).
- [9] C. R. Morton, D. J. Hinde, J. R. Leigh, J. P. Lestone, M. Dasgupta, J. C. Mein, J. O. Newton, and H. Timmers, *Phys. Rev. C* **52**, 243 (1995).
- [10] A. Saxena, A. Chatterjee, R. K. Choudhury, S. S. Kapoor, and D. M. Nadkarni, *Phys. Rev. C* **49**, 932 (1994).
- [11] R. Tripathi, K. Sudarshan, S. Sodaye, A. V. R. Reddy, K. Mahata, and A. Goswami, *Phys. Rev. C* **71**, 044616 (2005).
- [12] D. Hilscher, J. R. Birkelund, A. D. Hoover, W. U. Schroder, W. W. Wilcke, J. R. Huizenga, A. C. Mignerey, K. L. Wolf, H. F. Breuer, and V. E. Viola, *Phys. Rev. C* **20**, 576 (1979).
- [13] M. Thoennessen and G. F. Bertsch, *Phys. Rev. Lett.* **71**, 4303 (1993).
- [14] N. Bohr and J. A. Wheeler, *Phys. Rev.* **56**, 426 (1939).
- [15] J. Blocki, Y. Boneh, J. R. Nix, J. Randrup, M. Robel, A. J. Sierk, and W. J. Swiatecki, *Ann. Phys.* **113**, 330 (1978).
- [16] D. J. Hinde, H. Ogata, M. Tanaka, T. Shimoda, N. Takahashi, A. Shinohara, S. Wakamatsu, K. Katori, and H. Okamura, *Phys. Rev. C* **39**, 2268 (1989).
- [17] R. N. Sagaidak and A. N. Andreyev, *Phys. Rev. C* **79**, 054613 (2009).
- [18] V. Singh, B. R. Behera, M. Kaur, P. Sugathan, K. S. Golda, A. Jhingan, J. Sadhukhan, D. Siwal, S. Goyal, S. Santra, A. Kumar, R. K. Bhowmik, M. B. Chatterjee, A. Saxena, S. Pal, and S. Kailas, *Phys. Rev. C* **86**, 014609 (2012).
- [19] V. Singh, B. R. Behera, M. Kaur, A. Kumar, P. Sugathan, K. S. Golda, A. Jhingan, M. B. Chatterjee, R. K. Bhowmik, D. Siwal, S. Goyal, J. Sadhukhan, S. Pal, A. Saxena, S. Santra, and S. Kailas, *Phys. Rev. C* **87**, 064601 (2013).
- [20] R. Sandal, B. R. Behera, V. Singh, M. Kaur, A. Kumar, G. Singh, K. P. Singh, P. Sugathan, A. Jhingan, K. S. Golda, M. B. Chatterjee, R. K. Bhowmik, S. Kalkal, D. Siwal, S. Goyal, S. Mandal, E. Prasad, K. Mahata, A. Saxena, J. Sadhukhan, and S. Pal, *Phys. Rev. C* **87**, 014604 (2013).
- [21] D. J. Hinde, R. J. Charity, G. S. Foote, J. R. Leigh, J. O. Newton, S. Ogazaza, and A. Chattejee, *Nucl. Phys. A* **452**, 550 (1986).
- [22] J. O. Newton, D. J. Hinde, R. J. Charity, J. R. Leigh, J. J. M. Bokhorst, A. Chatterjee, G. S. Foote, and S. Ogaza, *Nucl. Phys. A* **483**, 126 (1988).
- [23] W. Ye, *Eur. Phys. J. A* **18**, 571 (2003).
- [24] W. Ye, *Phys. Rev. C* **79**, 031601(R) (2009).
- [25] R. Mahajan, B. R. Behera, M. Thakur, G. Kaur, P. Sharma, K. Kapoor, A. Kumar, P. Sugathan, A. Jhingan, A. Chatterjee, N. Saneesh, A. Yadav, R. Dubey, N. Kumar, H. Singh, A. Saxena, and S. Pal, *Phys. Rev. C* **98**, 034601 (2018).
- [26] H. Singh, A. Kumar, B. R. Behera, I. M. Govil, K. S. Golda, P. Kumar, A. Jhingan, R. P. Singh, P. Sugathan, M. B. Chatterjee, S. K. Datta, Ranjeet, S. Pal, and G. Vjesti, *Phys. Rev. C* **76**, 044610 (2007).
- [27] H. Singh, K. S. Golda, S. Pal, Ranjeet, R. Sandal, B. R. Behera, G. Singh, A. Jhingan, R. P. Singh, P. Sugathan, M. B. Chatterjee, S. K. Datta, A. Kumar, G. Vjesti, and I. M. Govil, *Phys. Rev. C* **78**, 024609 (2008).
- [28] C. Schmitt, K. Mazurek, and P. N. Nadtochy, *Phys. Rev. C* **97**, 014616 (2018).
- [29] M. Shareef, A. Chatterjee, and E. Prasad, *Eur. Phys. J. A* **52**, 342 (2016).

- [30] P. Sugathan, A. Jhingan, K. S. Golda, T. Varughese, S. Venkataramanan, N. Saneesh, V. V. Satyanarayana, S. K. Suman, J. Antony, R. Shanti, K. Singh, S. K. Saini, A. Gupta, A. Kothari, P. Barua, Rajesh Kumar, J. Zacharias, R. P. Singh, B. R. Behera, S. K. Mandal, I. M. Govil, and R. K. Bhowmik, *Pramana* **83**, 807 (2014).
- [31] K. S. Golda, A. Jhingan, P. Sugathan, H. Singh, R. P. Singh, B. R. Behera, S. Mandal, A. Kothari, A. Gupta, J. Zacharias, M. Archunan, P. Barua, S. Venkataramanan, R. K. Bhowmik, I. M. Govil, S. K. Datta, and M. B. Chatterjee, *Nucl. Instrum. Methods* **763**, 58 (2014).
- [32] M. Shareef, E. Prasad, A. Jhingan, N. Saneesh, K. S. Golda, A. M. Vinodkumar, M. Kumar, A. Shamlath, P. V. Laveen, A. C. Visakh, M. M. Hosamani, S. K. Duggi, P. S. Devi, G. N. Jyothi, A. Tejaswi, P. N. Patil, J. Sadhukhan, P. Sugathan, A. Chatterjee, and S. Pal, *Phys. Rev. C* **99**, 024618 (2019).
- [33] T. G. Masterson, *Nucl. Instrum. Methods* **88**, 61 (1970).
- [34] S. Venkataramanan, Arti Gupta, K. S. Golda, H. Singh, R. Kumar, R. P. Singh, and R. K. Bhowmik, *Nucl. Instrum. Methods Phys. Res. A* **596**, 248 (2008).
- [35] V. E. Viola, K. Kwiatkowski, and M. Walker, *Phys. Rev. C* **31**, 1550 (1985).
- [36] J. Sadhukhan, Ph.D thesis, Homi Bhabha National Institute, Mumbai, 2012.
- [37] P. Fröbrich and I. I. Gontchar, *Phys. Rep.* **292**, 131 (1998).
- [38] H. A. Kramers, *Physica (Amsterdam)* **7**, 284 (1940).
- [39] A. Bohr and B. R. Mottelson, *Nuclear Structure* (Benjamin, London, 1975), Vol. II.
- [40] E. G. Ryabov, A. V. Karpov, P. N. Nadtochy, and G. D. Adeev, *Phys. Rev. C* **78**, 044614 (2008).
- [41] A. J. Sierk, *Phys. Rev. C* **33**, 2039 (1986).
- [42] J. P. Lestone and S. G. McCalla, *Phys. Rev. C* **79**, 044611 (2009).
- [43] K. H. Bhatt, P. Grange, and B. Hiller, *Phys. Rev. C* **33**, 954 (1986).
- [44] H. Hofmann and J. R. Nix, *Phys. Lett. B* **122**, 117 (1983).
- [45] P. Grange, S. Hassani, H. A. Weidenmüller, A. Gavron, J. R. Nix, and A. J. Sierk, *Phys. Rev. C* **34**, 209 (1986).
- [46] H. Feldmeier, *Rep. Prog. Phys.* **50**, 915 (1987).
- [47] I. Mukul, S. Nath, K. S. Golda, A. Jhingan, J. Gehlot, E. Prasad, S. Kalkal, M. B. Naik, T. Banerjee, T. Varughese, P. Sugathan, N. Madhavan, and S. Pal, *Phys. Rev. C* **92**, 054606 (2015).
- [48] G. G. Chubaryan, M. G. Itkis, S. M. Luk'yanov, V. N. Okolovich, Yu. E. Penionzhkevich, A. Ya. Rusanov, V. S. Salamatin, and G. N. Smirenkin, *Yad. Fiz.* **56**, 3 (1993) [*Phys. At. Nucl.* **56**, 286 (1993)].
- [49] N. K. Rai, V. Mishra, and A. Kumar, *Phys. Rev. C* **98**, 024626 (2018).